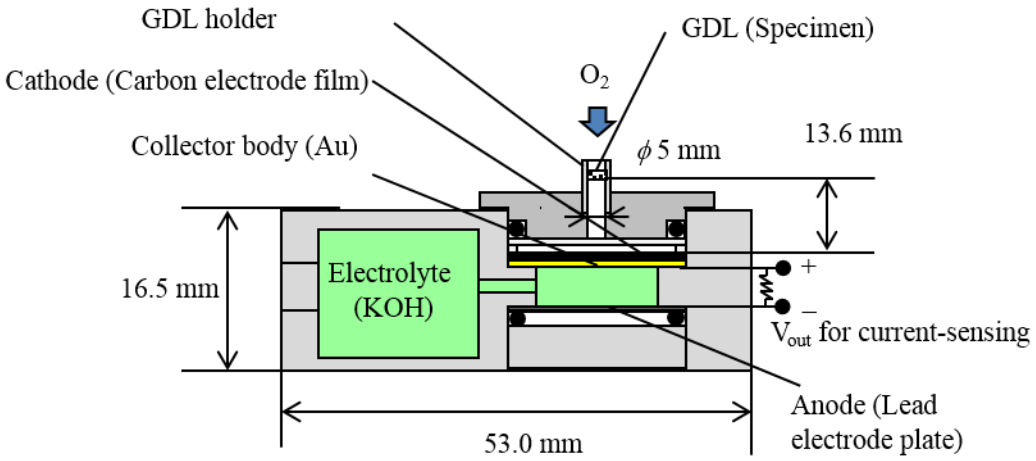

Fig. 1 Schematic diagram of galvanic cell oxygen absorber apparatus for oxygen diffusivity measurement for simultaneous measurement with X-ray imaging

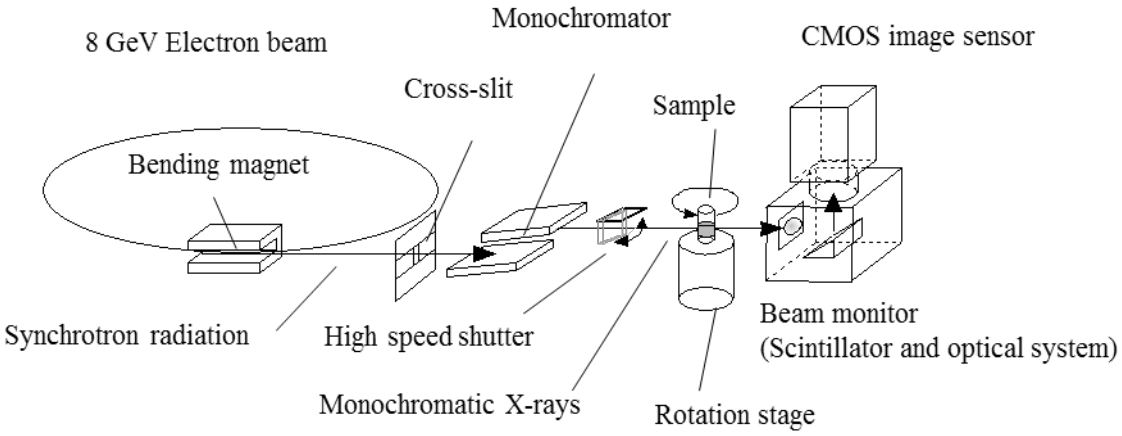

Fig. 2 Outline of projection tomographic X-ray system

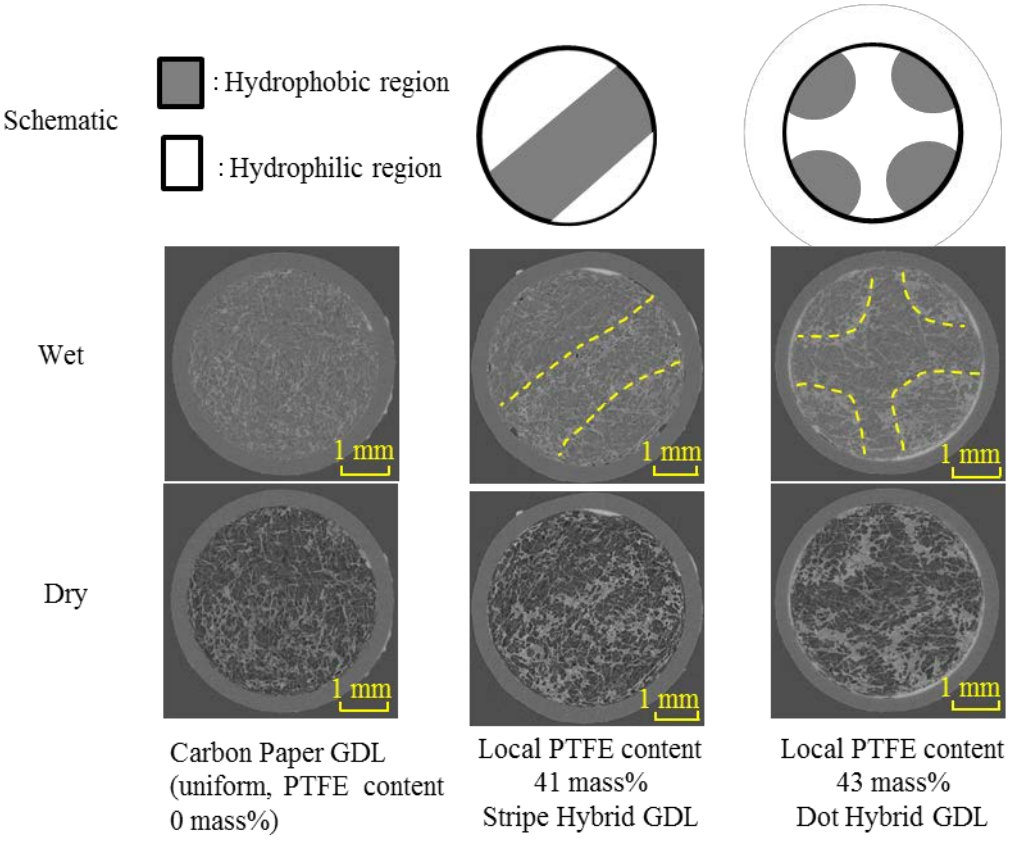

Fig. 3 Schematic diagrams and X-ray CT images of the GDLs

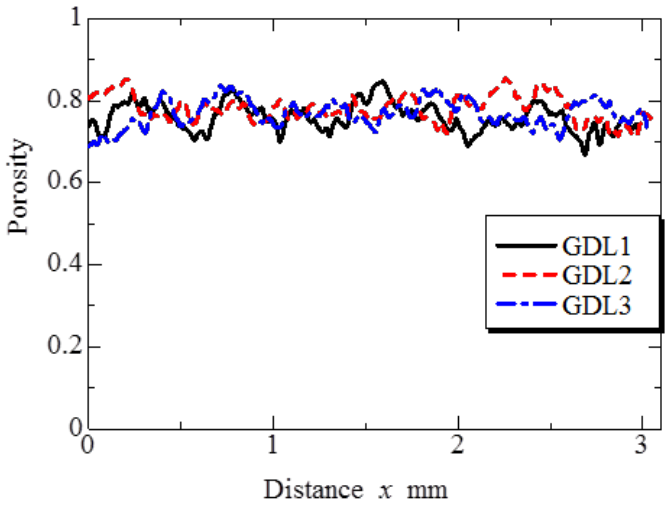

Fig. 4 Porosity distribution of untreated carbon paper GDL with 0 mass% PTFE content

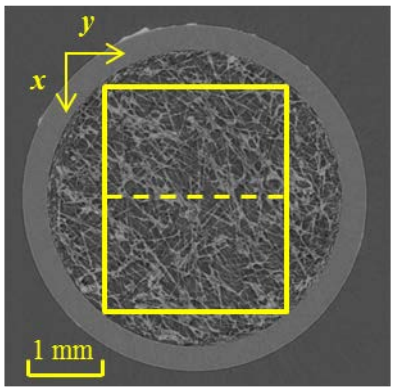

(a) Measurement area of CT

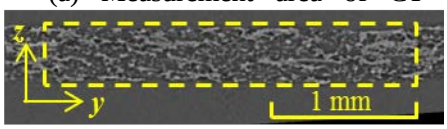

(b) Cross-sectional image.

Fig. 5 Measurement area of untreated carbon paper GDL with 0 mass% PTFE content

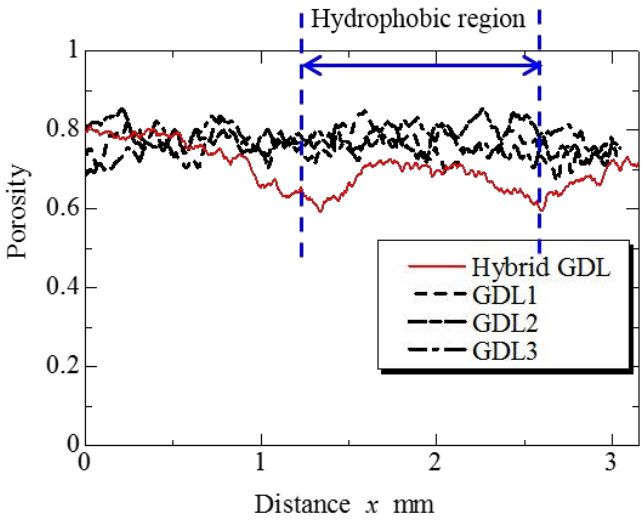

(a) Porosity distribution.

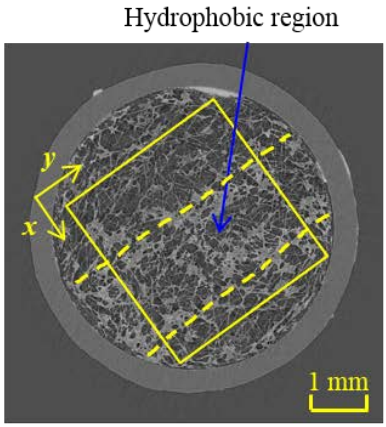

(b) Measurement area

Fig. 6 Porosity distribution and measurement area of stripe hybrid GDL (with non-uniform wettability distribution)

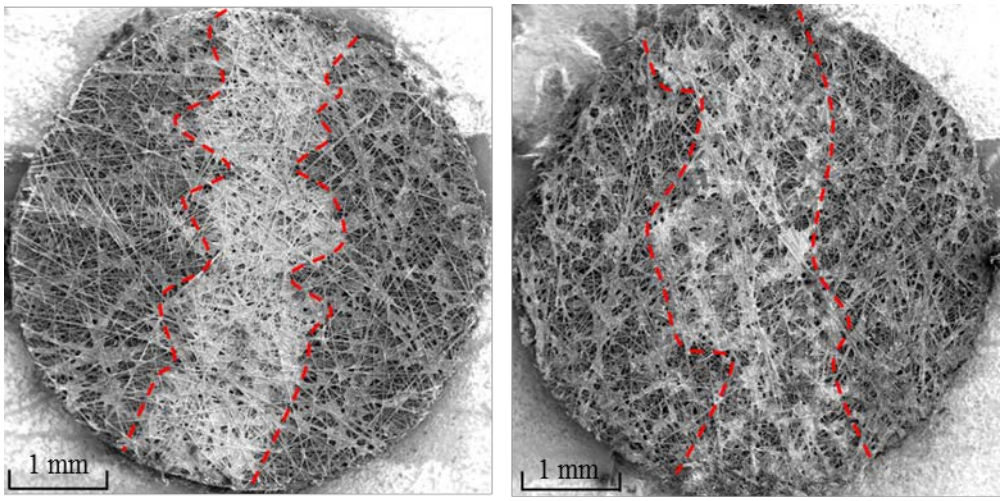

(a) Obverse side of hybrid GDL (b) Reverse side of hybrid GDL

Fig. 7 SEM micrographs of the surface morphology of the hybrid GDL

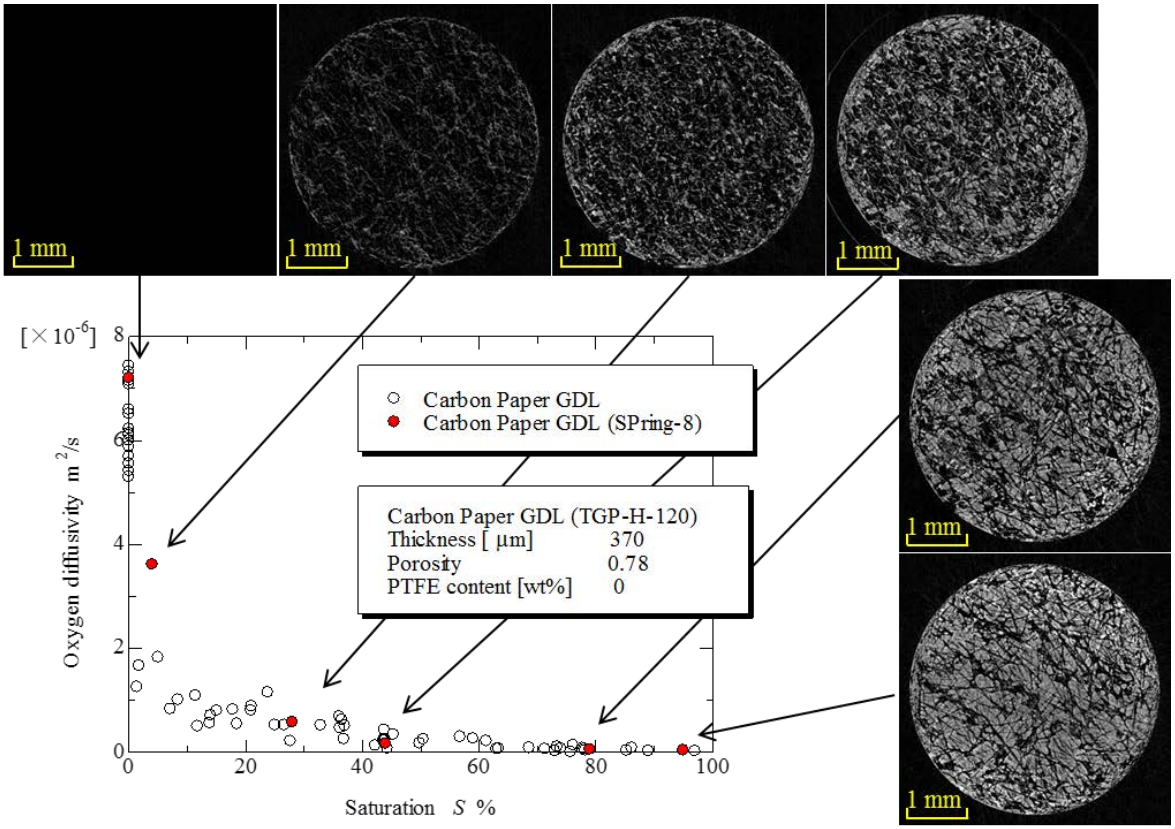

Fig. 8 Oxygen diffusivity as a function of the average saturation in untreated carbon paper GDL with 0 mass% PTFE content with corresponding CT images

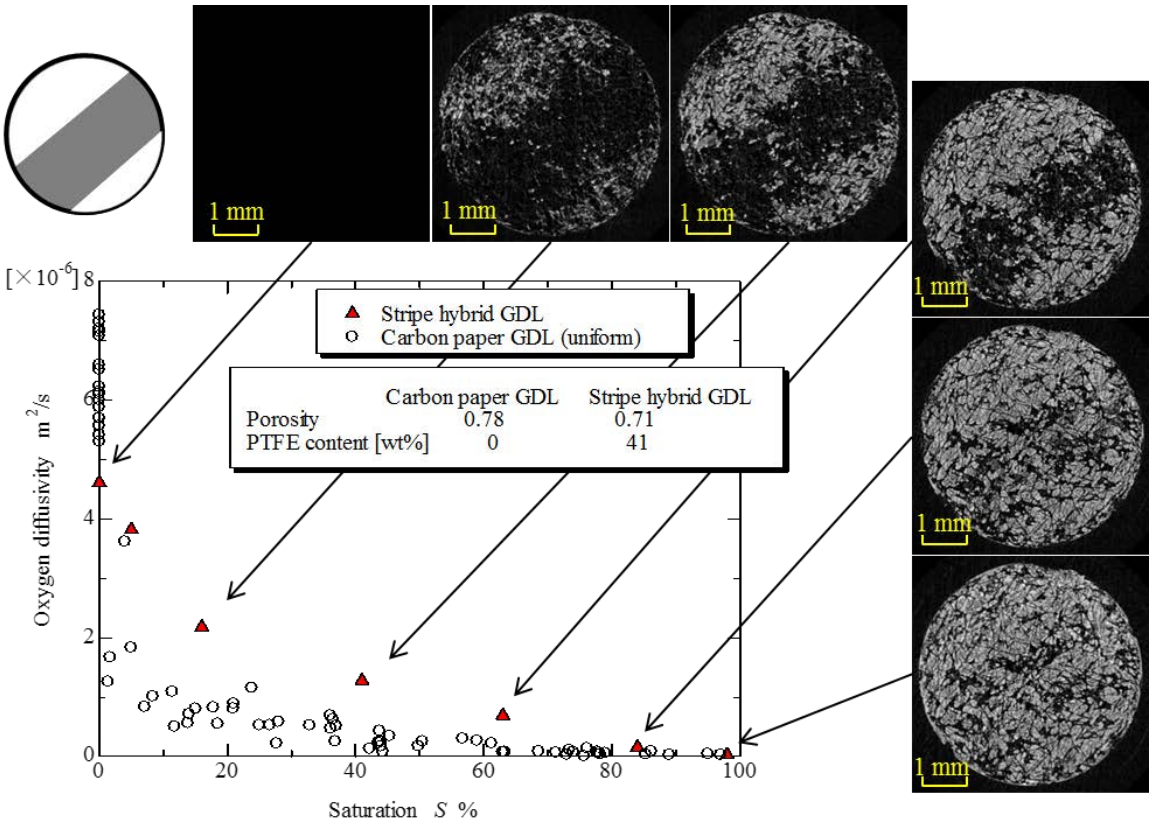

Fig. 9 Oxygen diffusivity in stripe hybrid GDL with non-uniform wettability distribution as a function of the average saturation with corresponding CT images

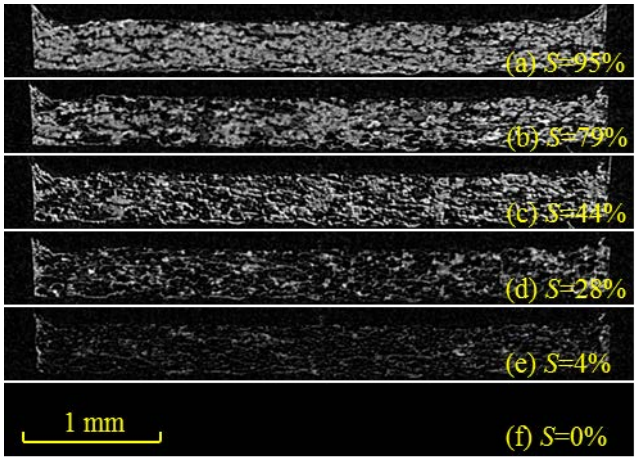

Fig. 10 Cross-sectional images of the untreated carbon paper GDL with 0 mass% PTFE content

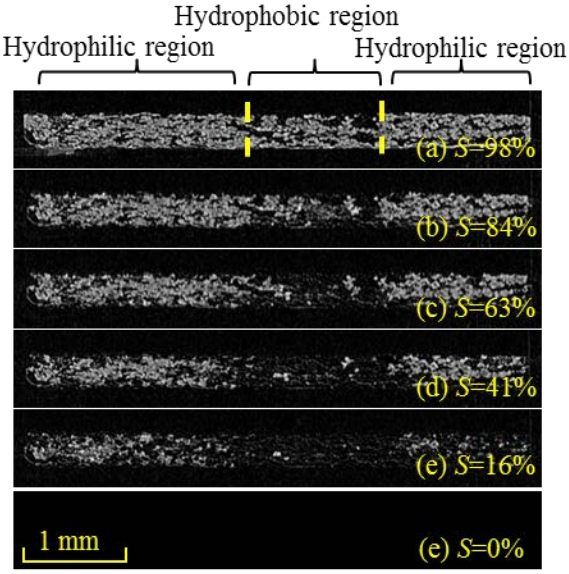

Fig. 11 Cross-sectional images of hybrid GDL with wettability distribution

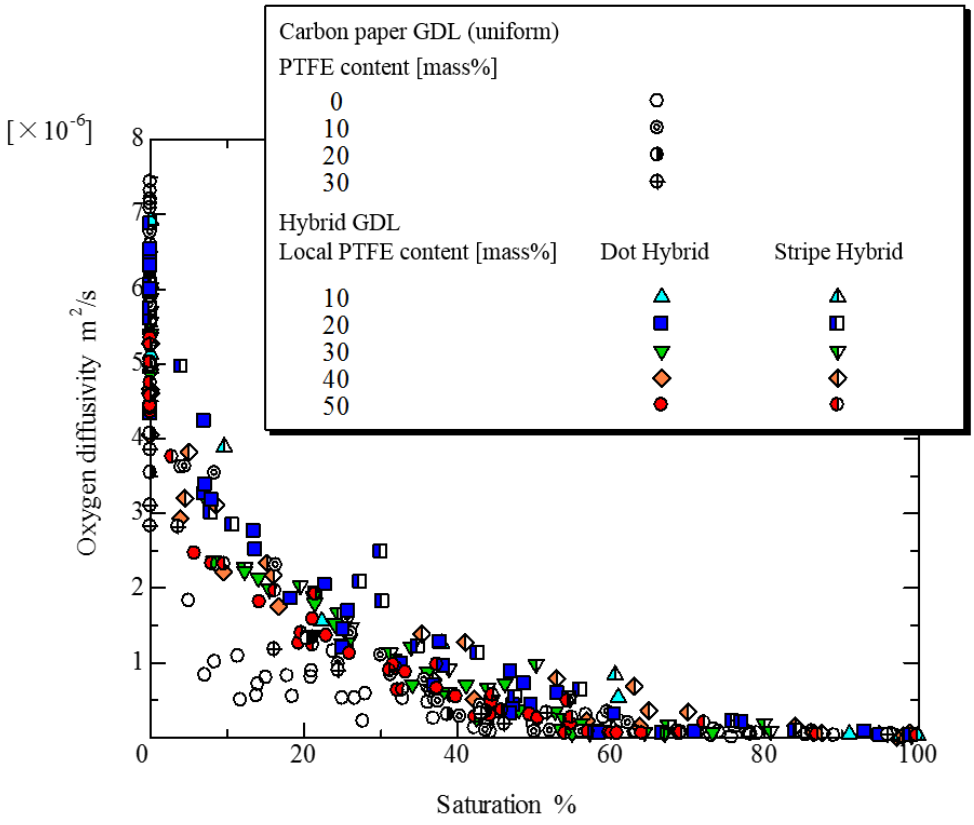

Fig. 12 Effective oxygen diffusivity as a function of the average saturation for various GDLs